Frontiers in Bioscience Landmark

Front. Biosci. (Landmark Ed) **2023**; 28(3): 55
https://doi.org/10.31083/j.fbl2803055

Original Research

The Consideration of Pseudoxanthoma Elasticum as a Progeria Syndrome

Janina Tiemann[1,†], Christopher Lindenkamp[1,†], Thomas Wagner[1], Andreas Brodehl[2], Ricarda Plümers[1], Isabel Faust-Hinse[1], Cornelius Knabbe[1], Doris Hendig[1,*]

[1]Institut für Laboratoriums- und Transfusionsmedizin, Herz- und Diabeteszentrum Nordrhein-Westfalen, Universitätsklinik der Ruhr-Universität Bochum, 32545 Bad Oeynhausen, Germany
[2]E. & H. Klessmann Institute for Cardiovascular Research & Development, Herz- und Diabeteszentrum Nordrhein-Westfalen, Universitätsklinik der Ruhr-Universität Bochum, 32545 Bad Oeynhausen, Germany
*Correspondence: dhendig@hdz-nrw.de (Doris Hendig)
[†]These authors contributed equally.
Academic Editor: Amancio Carnero Moya
Submitted: 27 July 2022 Revised: 1 December 2022 Accepted: 2 December 2022 Published: 20 March 2023

Abstract

Background: Pseudoxanthoma elasticum (PXE) is a rare autosomal recessive disorder caused by mutations in the *ATP-binding cassette sub-family C member 6* (*ABCC6*) gene. Patients with PXE show molecular and clinical characteristics of known premature aging syndromes, such as Hutchinson-Gilford progeria syndrome (HGPS). Nevertheless, PXE has only barely been discussed against the background of premature aging, although a detailed characterization of aging processes in PXE could contribute to a better understanding of its pathogenesis. Thus, this study was performed to evaluate whether relevant factors which are known to play a role in accelerated aging processes in HGPS pathogenesis are also dysregulated in PXE. **Methods**: Primary human dermal fibroblasts from healthy donors (n = 3) and PXE patients (n = 3) and were cultivated under different culture conditions as our previous studies point towards effects of nutrient depletion on PXE phenotype. Gene expression of *lamin A*, *lamin C*, *nucleolin*, *farnesyltransferase* and *zinc metallopeptidase STE24* were determined by quantitative real-time polymerase chain reaction. Additionally, protein levels of lamin A, C and nucleolin were evaluated by immunofluorescence and the telomere length was analyzed. **Results**: We could show a significant decrease of *lamin A* and *C* gene expression in PXE fibroblasts under nutrient depletion compared to controls. The gene expression of *progerin* and *farnesyltransferase* showed a significant increase in PXE fibroblasts when cultivated in 10% fetal calf serum (FCS) compared to controls. Immunofluorescence microscopy of *lamin A/C* and *nucleolin* and mRNA expression of *zinc metallopeptidase STE24* and *nucleolin* showed no significant changes in any case. The determination of the relative telomere length showed significantly longer telomeres for PXE fibroblasts compared to controls when cultivated in 10% FCS. **Conclusions**: These data indicate that PXE fibroblasts possibly undergo a kind of senescence which is independent of telomere damage and not triggered by defects of the nuclear envelope or nucleoli deformation.

Keywords: ABCC6; premature aging; progerin; lamin

1. Introduction

Pseudoxanthoma elasticum (PXE, MIM #264800) is a rare autosomal recessive disorder with an estimated prevalence between 1:25,000 and 1:100,000 and a female dominance for yet unknown reasons [1]. The main causes of PXE are mutations in the *ATP-binding cassette sub-family C member 6* (*ABCC6*) gene which lead to a deficiency of the encoded ABC-transporter protein [2,3]. The ABCC6 is primarily expressed in the liver, kidney and, to a lesser extent, in peripheral tissues, such as the skin. As the physiological substrate of the ABCC6 transporter is still unknown, the molecular understanding of PXE pathophysiology and the development of suitable treatments is complicated. Clinical manifestations of an ABCC6 transporter deficiency are an ectopic calcification due to mineralization and fragmentation of elastic fibers. This leads to arteriosclerosis, visual impairments with similarities to age-related macular degeneration and a premature loss of skin elasticity, which results in a strong wrinkle formation [1,4]. Although these clinical characteristics resemble those which can often be observed in older individuals, PXE has only been barely discussed in the context of premature aging.

This is even more surprising when considering that PXE shows molecular similarities to known premature aging syndromes, such as the Hutchinson-Gilford progeria syndrome (HGPS, MIM #176670). Thus, a study on progerin-overexpressing mice ($Lmna^{G609G/+}$ mice) which display clinical symptoms of HGPS patients showed a massive aortic calcification caused by an impaired pyrophosphate (PPi) homeostasis, including increased alkaline phosphatase activity as well as decreased plasma ATP and plasma pyrophosphate levels [5]. An increased alkaline phosphatase activity and decreased plasma ATP and plasma pyrophosphate level were also observed for PXE [6,7]. It was additionally shown that dermal fibroblasts from PXE and HGPS patients show a high activity of

senescence-associated beta-galactosidase and an increased expression of proinflammatory factors, which belong to the senescence-associated secretory phenotype [8,9]. A further study showed that a treatment with statins and bisphosphonates can extend the lifespan of *Zmpste24*$^{-/-}$ mice, another model mimicking HGPS [10]. A similar treatment was found to have beneficial effects in the case of PXE [11–13].

The HGPS is caused by a mutation in the *Lamin A* (*LMNA*) gene, which encodes an intermediate filament protein forming the nuclear lamina. The mutation activates a cryptic splice donor side leading to a mutant and truncated LMNA form, called progerin. However, an increased expression of progerin is not exclusive to HGPS but also happens during physiological aging [14]. The 50-amino acid deletion within progerin includes a PCYOX (ZMPSTE24) cleavage site, which is essential for the cleavage of the farnesyl group, the last step in LMNA maturation. The final cleavage of the farnesyl group is necessary for the correct anchoring of LMNA within the nuclear lamina. The missing ZMPSTE24 cleavage site results in the toxic permanent farnesylation of progerin and, therefore, the alteration and impairment of nuclear shape and integrity [15]. In addition to affecting the nuclear shape and stability, studies revealed that the increased expression of progerin may also affect other nuclear structures. Thus, dermal fibroblasts from HGPS patients show an increased size and a decreased number of nucleoli, which are important subcompartments of the nucleus. Enlarged nucleoli indicate an enhanced ribosome biogenesis and protein synthesis and are, thus, supposed to be a hallmark of aging [16,17].

The HGPS and the increased expression of progerin are also associated with an accelerated shortening of telomeres and telomere dysfunction [18,19]. Telomeres consist of tandem DNA repeats and are located at the ends of chromosomes to protect them from degradation. Telomeres become shorter in every cell division during physiological aging until they reach a critical length. At this critical length, cells undergo permanent cell cycle arrest to prevent further DNA damage [20]. The accelerated accumulation of these arrested cells contributes to the premature aging symptoms seen in HGPS [19].

It could be beneficial to investigate whether molecular factors involved in HGPS are also relevant for PXE because of the molecular similarities of PXE and HGPS. Thus, the aim of this study was to evaluate the expression of A-type lamins (LMNA, lamin C and progerin) and the gene expression of key enzymes of their processing, such as *ZMPSTE24* and the responsible *farnesyltransferase* (*FNTB*), in primary human dermal fibroblasts of PXE patients compared to healthy controls. Additionally, nucleolin (NCL) expression and telomere length were tested to get further insights into the nuclear integrity of nuclear structures of PXE fibroblasts.

2. Material and Methods

2.1 Experimental Design

The study was designed to evaluate relevant factors known to be involved in HGPS pathogenesis in primary human dermal fibroblasts of PXE patients. Fibroblasts from PXE patients (n = 3) and healthy age- and gender-adjusted donors (n = 3) were cultured in medium with 10% fetal calf serum (FCS) or 10% lipoprotein deficient FCS (LPDS). This was done because a previous study had shown that lipid metabolism might play an important role in PXE pathogenesis [21]. Thus, the usage of LPDS should, on the one hand, trigger the endogenous cholesterol biosynthesis and, on the other hand, avoid any diminishment of the pathophysiological characteristics of PXE fibroblasts *in vitro* by an excess of exogenous cholesterol/lipoproteins. The gene expression of *LMNA*, *lamin C* and *progerin* and of the important factors of LMNA processing, *ZMPSTE24* and *FNTB*, were measured by quantitative real-time polymerase chain reaction (qPCR) for analysis. Additionally, the mRNA expression of *NCL*, one of the most abundant proteins in nucleoli, was determined to further evaluate the nuclear organization in PXE fibroblasts. A-type lamins and NCL were also investigated by immunofluorescence microscopy. Furthermore, the relative telomere length of PXE fibroblasts compared to the control was examined.

2.2 Cell Culture

Normal human dermal fibroblasts (NHDF) were purchased from the Coriell Institute for Medical Research (Camden, USA). Dermal fibroblasts from PXE patients were isolated from skin biopsies. Details about fibroblasts characteristics can be found in **Supplementary Table 1**.

Fibroblasts were cultivated in Dulbecco's modified essential medium (31053044, Gibco, Thermo Fisher Scientific, Santa Fe, NM, USA) containing 10% FCS (S181G-500, Biowest, Nuaillé, France), 2% L-glutamine (200 mM) (P04-80100, PAN Biotech, Aichenbach, Germany) and 1% antibiotic/antimycotic solution (P0607300, PAA Laboratories, Pasching, Austria). Fibroblasts were subcultured when they reached confluency.

Fibroblasts between passage 9 and 12 were used and biological samples were prepared in triplicate for all experiments performed. Fibroblasts were seeded in a final cell density of 177 cells/mm^2 in 60 mm culture dishes (353004, BD Falcon, Franklin Lakes, NJ, USA) for qPCR and telomere length analysis. They were cultured for 24 h in 10% FCS. Afterwards, medium was changed to fresh 10% FCS or 10% LPDS for an additional 24 h. Coverslips (ø 18 mm) were coated with 5 μg/cm^2 rat collagen (50202, Ibidi, Martinsried, Germany) and placed into a 12-well plate (665180, Greiner bio-one, Frickenhausen, Germany) for immunofluorescence experiments. Cells were seeded with a final cell density of 177 cells/mm^2 and incubated for 24 h in 10% FCS. Medium was subsequently replaced by fresh 10% FCS or 10% LPDS for a further 72 h.

2.3 Delipidation of FCS

The LPDS was prepared as described by Gibson *et al.* [22]. In brief, 1 g Cab-o-sil (silicic acid powder) (112945-52-5, Spectrum Chemical Mfg. Corp., New Brunswick, NJ, USA) was added to 50 mL FCS and stored at 4 °C overnight. Subsequently, mixtures were centrifuged for 1 h at 4 °C and 5000 × g. The supernatants were stored at –20 °C until further use. Before medium preparation, LPDS was sterile filtered (0.2 μm). The delipidation of FCS lowered the free cholesterol by about 78%, low-density lipoprotein (LDL) by about 95% and high-density lipoprotein (HDL) by about 57%. Triglyceride concentrations remained unchanged.

2.4 Nucleic Acid Isolation

NucleoSpin RNA Kit (740955250, Macherey-Nagel, Düren, Germany) was used for the RNA isolation according to the manufacturer's instructions. DNA isolation for the analysis of the telomere length was performed using the NucleoSpin Blood extraction Kit (740951, Macherey-Nagel, Düren, Germany).

2.5 Gene Expression Analysis

A volume of 1 μg total RNA was transcribed into cDNA using SuperScript II Reverse Transcriptase (18064071, Thermo Fisher Scientific, Waltham, MA, USA). An amount of 2.5 μL cDNA (1:10), 0.25 μL forward and reverse primer (Biomers, Ulm, Germany), 2.0 μL water and 5.0 μL LightCycler 480 SYBR Green I Master reaction mixture (4707516001, Roche, Mannheim, Germany) was mixed for each measurement of *NCL*, *ZMPSTE24* and *FNTB*. The qPCR protocol involves an initial incubation for 5 min at 95 °C and an additional 45 cycles of denaturation (95 °C, 10 s), annealing (specific annealing temperature, 15 s) and elongation (72 °C, 20 s). The relative mRNA expression levels of these targets were normalized to relative *β-actin*, *glycerinaldehyd-3-phosphat-dehydrogenase* and *β2-microglobulin* mRNA expression. Finally, a melting curve analysis was done. Probes (5'- FAM and 3'- non-fluorescent quencher dye) (Thermo Fisher Scientific, Santa Fe, NM, USA) were designed according to the previous description of Rodriguez *et al.* [23] for the separate analysis of the gene expression of *LMNA*, *lamin C* and the *progerin* primer (Biomers, Ulm, Germany) and taqman minor groove binder. The relative mRNA expression levels of *LMNA*, *lamin C* and *progerin* were normalized to relative *β-glucuronidase* and *ribosomal protein large P0* mRNA expression. Validated taqman assays (5'- VIC and 3'- non-fluorescent quencher dye) were used (4316034, Thermo Fisher Scientific, Santa Fe, NM, USA) for the analysis of *β-glucuronidase* and *ribosomal protein large P0*. qPCR protocol and reaction mixtures were basically conducted as described by Rodriguez *et al.* [23], but reaction volumes were reduced to 10 μL, including 2.5 μL of template. Measurements were conducted using LightCycler 480 (Roche, Mannheim, Germany). The protocol for qPCR included 2 min (50 °C), 19 min (95 °C) and, subsequently, 50 cycles of 15 s (95 °C) and 40 s (60 °C). Results for gene expression analyses were calculated using the $\Delta\Delta$ Ct method considering the PCR efficiency. Technical triplicates were performed for each biological sample. Primer sequences and taqman minor groove binder probes used for qPCR can be found in **Supplementary Table 2**.

2.6 Immunofluorescence Microscopy

Microscopy cells were washed with phosphate-buffered saline (PBS; P04360010B, Gibco, Thermo Fisher Scientific, Germany) for immunofluorescence. Fibroblasts were fixed and permeabilized by incubating with acetone:methanol (1:1) for 10 min at room temperature. After two further washing steps with PBS, unspecific binding sites were blocked for 1 h in 1% bovine serum albumin diluted in PBS. Fibroblasts were washed twice and incubated afterwards with primary antibodies for 2 h at room temperature. Primary antibodies used included rabbit anti-lamin a/c (ab108595; Abcam, Cambridge, United Kingdom; 1:500), mouse anti-progerin (ab66587; Abcam, Cambridge, United Kingdom; 1:10) and mouse anti-NCL (ab13541, Abcam, Cambridge, United Kingdom; 1:500). After two additional washing steps, the cells were incubated with secondary antibodies for 1 h at room temperature under the exclusion of light. Secondary antibodies used were fluorescein isothiocyanate-conjugated goat anti-rabbit (AB_2337975, Jackson Immuno Research, Cambridge, United Kingdom; 1:75) and tetramethylrhodamine-conjugated goat anti-mouse (AB_2338703, Jackson Immuno Research, Cambridge, United Kingdom; 1:75). All antibodies were diluted in 0.1% bovine serum albumin in PBS. After incubation, cells were again washed twice and counterstained with 4′,6-diamidino-2-phenylindole. After another three washing steps, coverslips were mounted with ProLong Diamond Antifade Mountant (P36961, Thermo Fisher Scientific, Santa Fe, NM, USA). Immunofluorescence images were captured by confocal laser scanning microscopy (Leica Microsystems, Wetzlar, Germany). The fluorescein isothiocyanate was excited at 488 nm and emission was detected between 493 and 557 nm. The tetramethylrhodamine was excited at 552 nm and emission was detected between 557 and 737 nm. Six pictures per cell culture condition were analyzed for the assessment of immunofluorescence images by using the software ImageJ ver.1.53 (Wayne Rasband, NIH, Bethesda, MD, USA). The area of nuclei was bordered and the intensity was measured. The area/intensity was calculated for all experimental conditions, and differences between PXE and controls were compared.

2.7 Relative Telomere Length

The DNA isolation was done as described previously. The determination of the relative telomere length was performed using the Relative Human Telomere Length Quan-

tification qPCR Assay Kit (#8908, ScienCell, Carlsbad, CA, USA). The primer available binds on any specific region on telomeres because they consist of repetitive sequences. In the case of a multiple binding of the primer to telomere, the DNA-polymerase remove those by their specific exonuclease activity. An amount of 2.5 μL DNA (3 ng/μL) was mixed with 10 μL LightCycler 480 SYBR Green I Master reaction mixture (4707516001, Roche, Mannheim, Germany), 5.5 μL water and 2.0 μL of either the telomere or the SCR primer set for the final measurement. Measurements were performed using LightCycler 480 (Roche, Mannheim, Germany). The protocol for this was divided into initial denaturation (10 min, 95 °C), 32 cycles of denaturation (20 s, 95 °C), annealing (20 s 52 °C), elongation (45 s 72 °C) and generation of a melting curve for 15 min (65–97 °C). The SCR primer supplied was used for normalization; it generates an amplificon with a length of 100 bp. The $\Delta\Delta$ Ct method was used for the calculation of the relative telomere length.

2.8 Statistical Analysis

Data of gene expression analyses and the relative telomere length are shown as mean $\pm$ standard error (SEM). GraphPad Prism 5.0 (GraphPad Software Inc., San Diego, CA, USA) was used as the statistical software. The non-parametric two-tailed Mann-Whitney U test was performed and p-values of 0.05 or less were considered statistically significant for all analyses.

3. Results

3.1 The Gene Expression of A-Type Lamins Altered but There Were No Significant Changes in Protein Expression or Distribution

The gene expression of *LMNA* and *lamin C* showed no significant changes of PXE fibroblasts compared to NHDF when cultured in 10% FCS, as seen in Fig. 1A,B. Under lipoprotein deficient conditions, *LMNA* (control: 0.85 $\pm$ 0.10, PXE: 0.50 $\pm$ 0.05; $p < 0.001$) and *lamin C* (control: 0.50 $\pm$ 0.07, PXE: 0.30 $\pm$ 0.04; $p < 0.01$) mRNA expression was significantly decreased in PXE fibroblasts compared to controls under the same conditions. Furthermore, *LMNA* (PXE in 10% FCS: 0.76 $\pm$ 0.06, PXE in 10% LPDS: 0.50 $\pm$ 0.05; $p < 0.01$) and *lamin C* (PXE in 10% FCS: 0.54 $\pm$ 0.05, PXE in 10% LPDS: 0.30 $\pm$ 0.04, $p < 0.001$) gene expression of PXE fibroblasts cultured in 10% LPDS were decreased compared to PXE fibroblasts cultured in 10% FCS. The appropriate controls showed no significant changes in *LMNA* and *lamin C* gene expression under the different conditions. Regarding the *progerin* mRNA expression (Fig. 1C), a significant increase in PXE fibroblasts compared to NHDF was seen under conditions with 10% FCS (control: 0.87 $\pm$ 0.12, PXE: 1.72 $\pm$ 0.30; $p < 0.05$). No changes in the *progerin* gene expression between the control and PXE fibroblast were seen when cultured in lipoprotein-deficient medium. Accordingly, PXE fibroblasts showed a significant decrease in *progerin* mRNA expression when cultured in medium with 10% LPDS compared to the cultivation in 10% FCS (PXE in 10% FCS: 1.72 $\pm$ 0.30, PXE in 10% LPDS: 0.77 $\pm$ 0.14, $p < 0.01$).

Immunofluorescence microscopy of LMNA/lamin C showed, despite minor variations which could be detected for every cell line, no grave alterations in protein expression, as can be seen in Fig. 2. Additionally, nuclei of PXE fibroblasts did not show any severe obvious deformation. Immunofluorescence analysis of progerin was not possible because the protein concentrations were too low to be reliably detected.

3.2 Alteration of Gene Expression of LMNA-Processing Enzymes

The gene expression of *FNTB* and *ZMPSTE24* was determined for the evaluation of putative alterations in LMNA/lamin C processing (Fig. 3). A significant increase was seen for PXE fibroblasts cultivated in medium with 10% FCS compared to NHDF (control: 1.08 $\pm$ 0.06, PXE: 1.54 $\pm$ 0.13, $p < 0.05$) for *FNTB* mRNA expression. No changes were detected for PXE fibroblasts cultured in lipoprotein-deficient medium compared to controls under the same conditions, and between the control fibroblasts in 10% FCS and 10% LPDS. Moreover, the *FNTB* gene expression was significantly decreased in PXE fibroblasts cultured in 10% LPDS when compared to cultivation in 10% FCS (PXE in 10% FCS: 1.54 $\pm$ 0.13, PXE in 10% LPDS: 1.15 $\pm$ 0.11, $p \leq 0.05$). No significant changes were seen for *ZMPSTE24* gene expression in any case.

3.3 Significant Changes of the Relative Telomere Length but no Changes in the Nucleoli Formation in PXE Fibroblasts

The *NCL* gene and protein expression did not show any significant changes either between the control and PXE fibroblasts or between the different cultivation media, as seen in Fig. 4A,B. The relative telomere length of PXE fibroblasts (Fig. 4C) was significantly longer compared to NHDF when cultured in medium with 10% FCS (control: 1.61 $\pm$ 0.15, PXE: 2.18 $\pm$ 0.16; $p < 0.01$). No significant changes between PXE fibroblasts and control fibroblasts were seen under lipoprotein deficient conditions. However, a significant reduction in the relative telomere length was detected for PXE fibroblasts cultured in medium with 10% LPDS compared to those cultured in medium with 10% FCS (PXE in 10% FCS: 2.18 $\pm$ 0.16, PXE in 10% LPDS: 1.66 $\pm$ 0.13, $p < 0.01$). No changes were seen for control fibroblasts between the different media.

4. Discussion

Pseudoxanthoma elasticum is a rare autosomal recessive disorder. Patients affected by PXE display clinical symptoms which resemble those seen in older individuals. Accordingly, PXE also shares some molecular characteris-

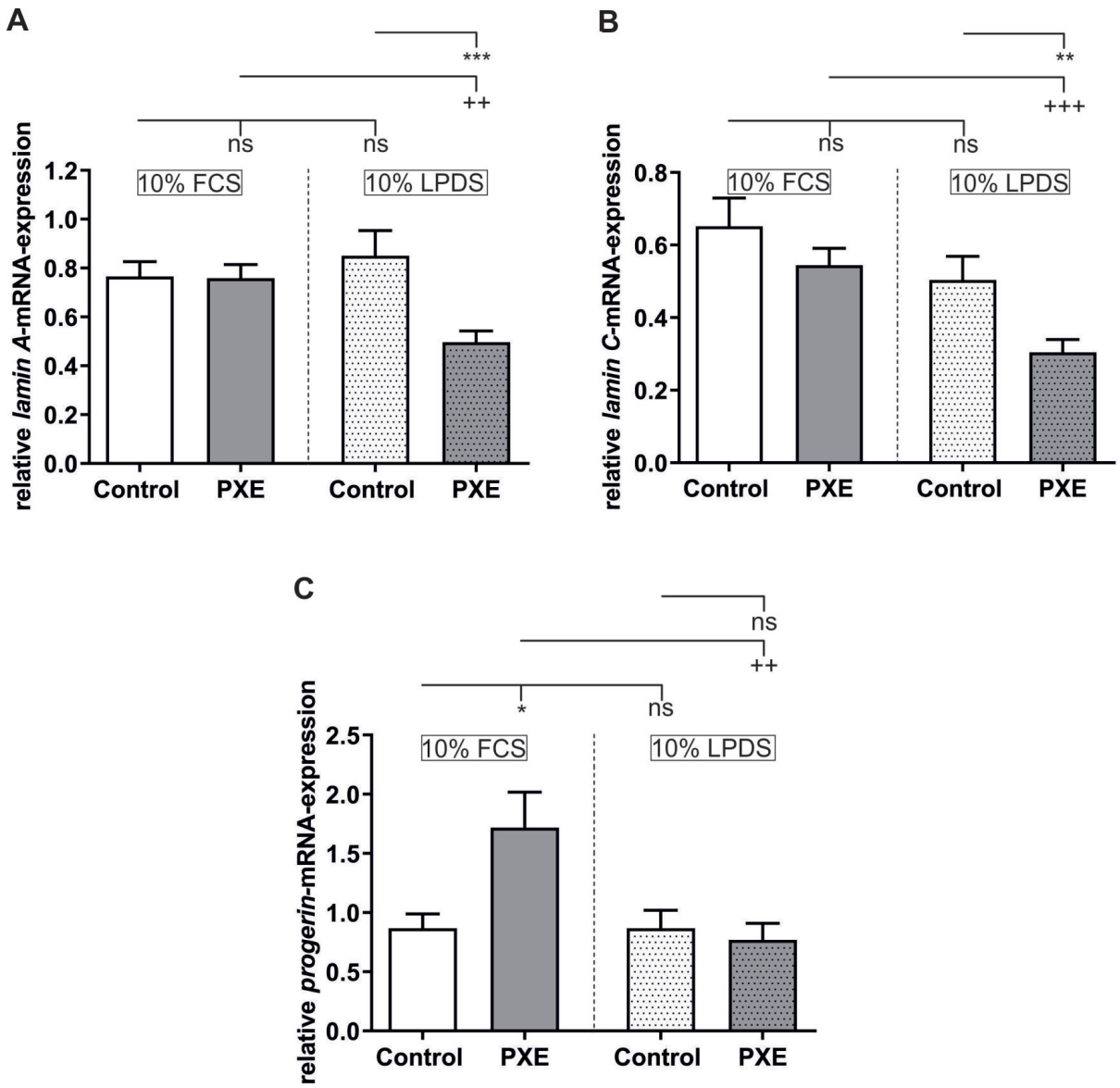

Fig. 1. Relative gene expression of A-type lamins. (A) Relative *lamin A* (*LMNA*) mRNA expression of PXE fibroblasts (grey, n = 3) and NHDF (white, n = 3). (B) Relative *lamin C* mRNA expression of PXE fibroblasts (grey, n = 3) and NHDF (white, n = 3). (C) Relative *progerin* mRNA expression of PXE fibroblasts (grey, n = 3) and NHDF (white, n = 3). Data are shown as mean ± SEM. Control vs. PXE: * $p \leq 0.05$; ** $p \leq 0.01$; *** $p \leq 0.001$; ns $p > 0.05$. 10% FCS vs. 10% LPDS: ++ $p \leq 0.01$; +++ $p \leq 0.001$; ns $p > 0.05$.

tics with the premature aging syndrome HGPS [5,10–13]. Although these facts are rather obvious, premature aging processes have only barely been connected to PXE pathogenesis to date. Thus, this study was performed to evaluate premature aging factors which are known to contribute to accelerated aging in HGPS patients in primary human dermal fibroblasts of PXE patients. Hereby, new insights into PXE pathogenesis could be revealed.

The disease-causing factor of HGPS is mostly a *de novo* mutation in the *LMNA* gene. This activates a cryptic splice donor side which leads to a mutant form of LMNA called progerin [14]. We found no significant increase in the mRNA expression for the *LMNA* splice variants *LMNA* and *lamin C* but a significant increase in the mRNA expression of *progerin* in PXE fibroblasts compared to NHDF when cultivated in 10% FCS. This is in accordance with data from Rodriguez *et al.* [23] showing no differences in *LMNA* or *lamin C* gene expression between the control and HGPS fibroblasts, although *progerin* mRNA expression was drastically increased in HGPS. We further analyzed the gene expression of the LMNA-processing enzymes *FNTB* and *ZMPSTE24*. The mRNA expression for *FNTB* showed a significant increase comparable to the *progerin* induction observed in PXE fibroblasts compared to NHDF when cultivated in 10% FCS (Fig. 5, Ref. [5,21,24,25]). The *FNTB* encodes a farnesyltransferase whose substrate is farnesyl

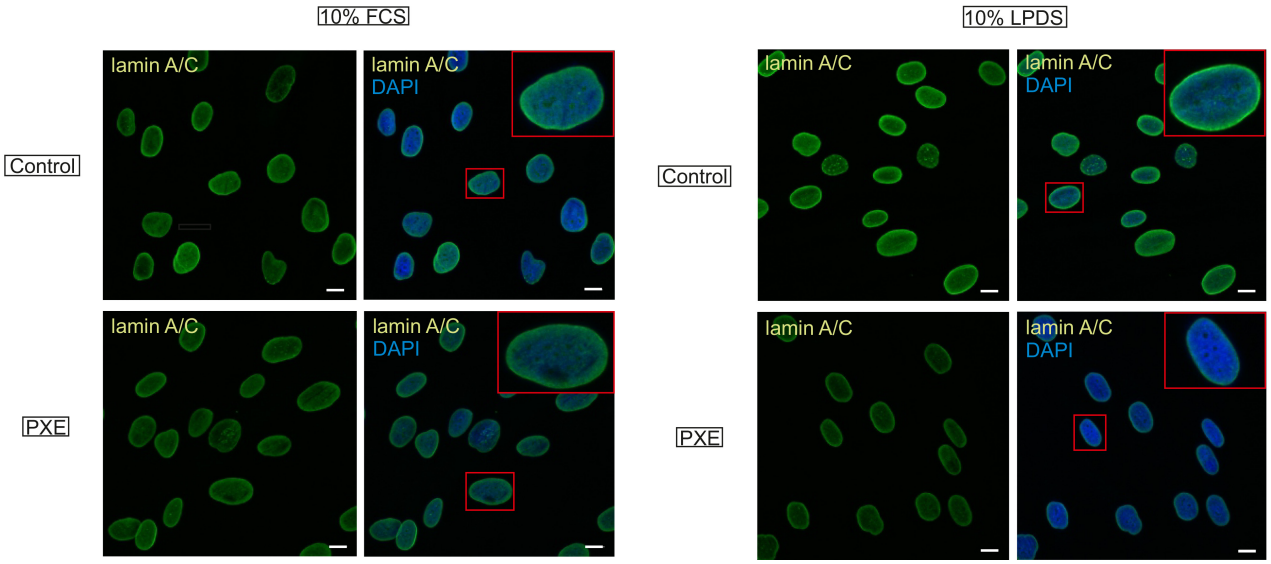

Fig. 2. Confocal laser scanning microscopy of LMNA/lamin C. Immunofluorescence analysis of LMNA/lamin C (green) was conducted in NHDF (n = 3) and PXE fibroblasts (n = 3) cultured in 10% FCS and 10% LPDS. Cells were counterstained with 4′,6-diamidino-2-phenylindole (DAPI, blue). Representative images are shown. Scale bar: 10 μm.

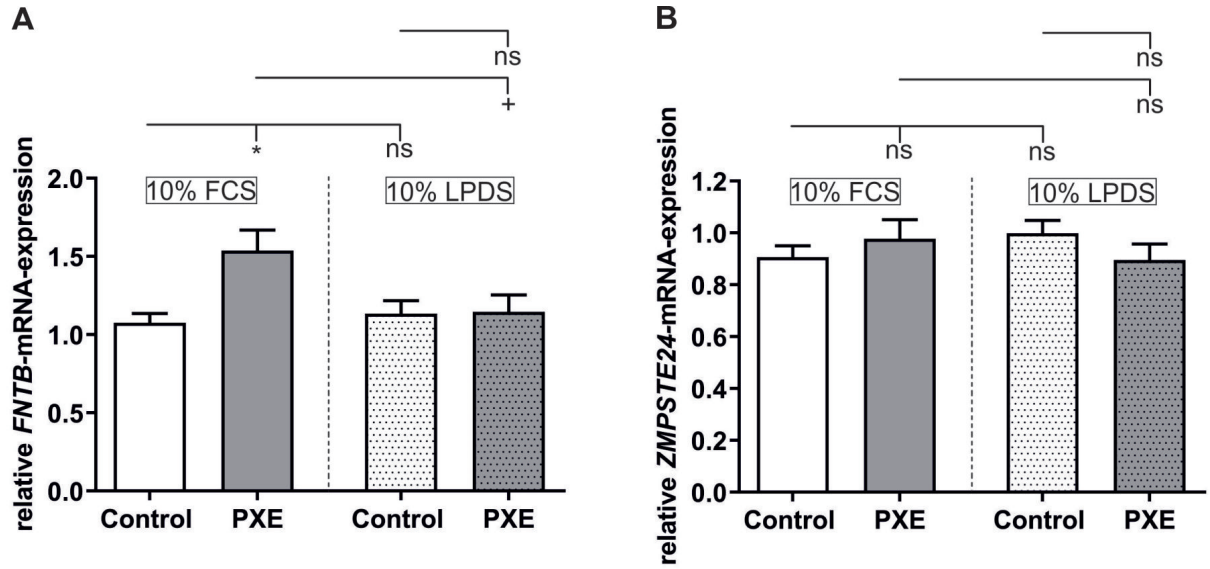

Fig. 3. Relative gene expression of *FNTB* and *ZMPSTE24*. (A) Relative *FNTB* mRNA expression of PXE fibroblasts (grey, n = 3) and NHDF (white, n = 3). (B) Relative *ZMPSTE24* mRNA expression of PXE fibroblasts (grey, n = 3) and NHDF (white, n = 3). Data are shown as mean ± SEM. Control vs. PXE: * $p \leq 0.05$; ns $p > 0.05$. 10% FCS vs. 10% LPDS: + $p \leq 0.05$; ns $p > 0.05$.

diphosphate, an intermediate of the cholesterol biosynthesis [26]. A previous study by Kuzaj *et al.* [21] showed that, although the 3hydroxy-3-methyl-glutaryl-coenzyme A reductase activity is increased in PXE fibroblasts, the gene expression of farnesyl diphosphate synthase, responsible for the conversion of isopentenyl diphosphate to farnesyl diphosphate, remained unchanged under conditions of 10% FCS. An induction of *FNTB* gene expression in PXE fibroblasts is, therefore, probably not directly a result of an excess supply of farnesyl diphosphate but could, nevertheless, possibly contribute to the increased formation of permanently farnesylated progerin. In contrast to the induction of *FNTB* gene expression, we found no changes in the mRNA expression for *ZMPSTE24* in PXE fibroblasts compared to controls when cultivated in 10% FCS. Because ZMPSTE24 is responsible for the cleavage of the 15 C-terminal amino acids of pre-LMNA, mice carrying a *Zmpste24* knockout are often used as models for HGPS as they show an accumu-

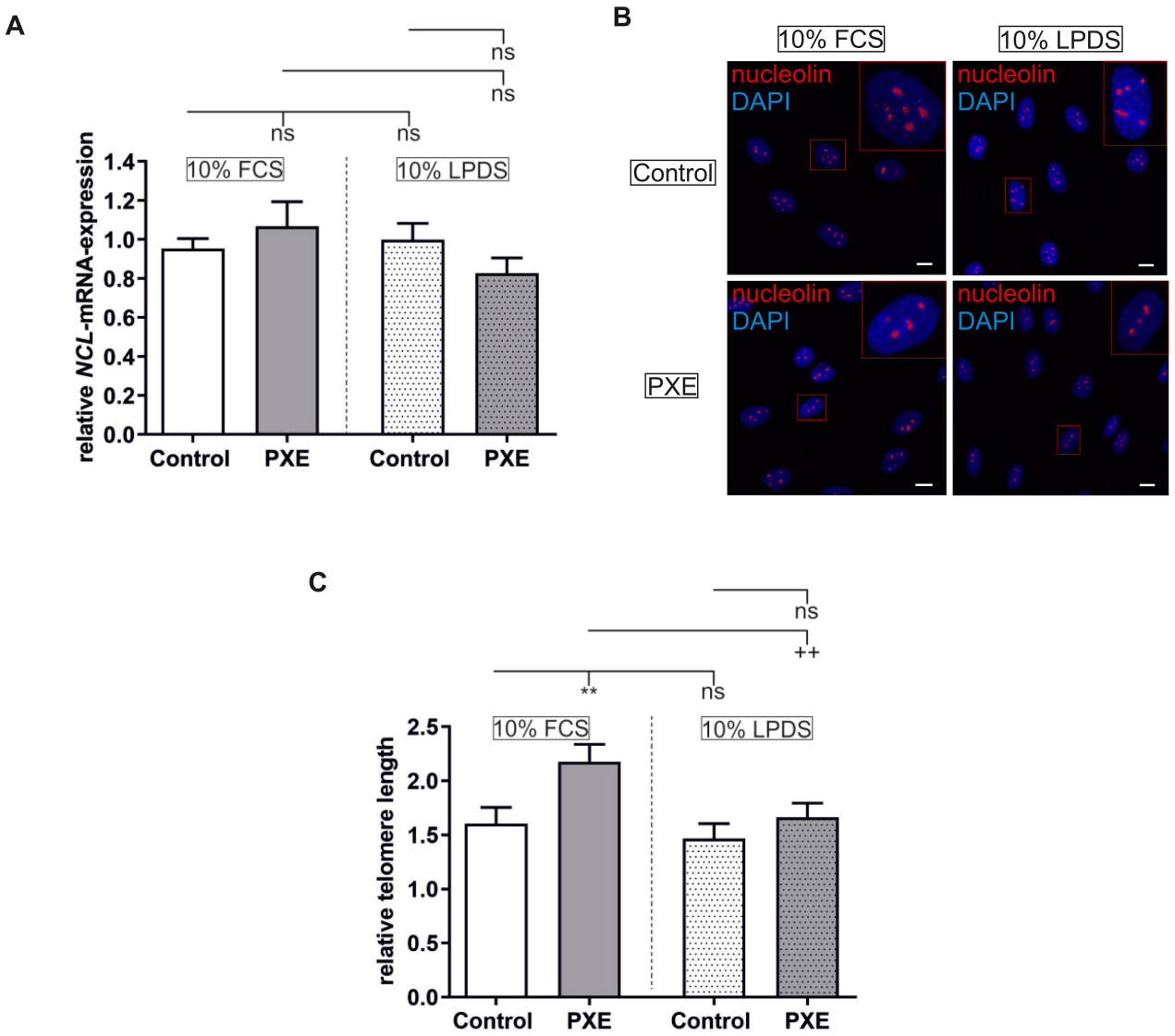

Fig. 4. Relative *nucleolin (NCL)* gene and protein expression and relative telomere length. (A) Relative *NCL* mRNA expression of PXE fibroblasts (grey, n = 3) and NHDF (white, n = 3). (B) Confocal laser scanning microscopy of NCL. Immunofluorescence analysis of NCL (red) was conducted in NHDF (n = 3) and PXE fibroblasts (n = 3) cultured in 10% FCS and 10% LPDS. Cells were counterstained with 4′,6-diamidino-2-phenylindole (blue). Representative images are shown. Scale bar: 10 μm. (C) Relative telomere length of PXE fibroblasts (grey, n = 3) and NHDF (white, n = 3). Data are shown as mean ± SEM. Control vs. PXE: ** $p \leq 0.01$; ns $p > 0.05$. 10% FCS vs. 10% LPDS: ++ $p \leq 0.01$; ns $p > 0.05$.

lation of unprocessed and, thus, permanently farnesylated pre-LMNA which has similar destructive effects to progerin [10]. As *ZMPSTE24* gene expression showed no simultaneous induction with the induction of the *FNTB* mRNA expression in PXE fibroblasts, this might lead to an increased occurrence of permanently farnesylated pre-LMNA. Accordingly, Kuzaj *et al*. [21] also showed that the prenylcysteine oxidase 1 (PCYOX) responsible for the degradation of prenylated proteins, such as LMNA or progerin, is also induced in PXE fibroblasts when cultivated in 10% FCS. Further studies indicate an association of PXE pathogenesis with the DNA damage response and poly (ADP-ribose) pathway [27]. It is also known that farnesylated pre-LMNA increases DNA damage and reduces defective DNA repair in HGPS. Increased *FNTB* and *PCYOX* gene expression in PXE fibroblasts might indicate an increased prenylation of proteins and, consequently, an increased need for their degradation. However, HGPS fibroblasts which show a clear progeroid phenotype display an up to 500 times induction of *progerin* gene expression [23], therefore, it is unlikely that a doubling of *progerin* mRNA expression, as seen here for PXE fibroblasts, or a slight potential accumulation of permanent farnesylation pre-LMNA have a major impact on PXE pathogenesis. This assumption is

strengthened by the fact that immunofluorescence analysis of LMNA/lamin C did not show any obvious changes of nuclei shape or aberrant distribution of lamins (Fig. 5).

As mentioned previously, studies showed that cholesterol biosynthesis plays an important role in PXE pathogenesis [21,28] and the supply of farnesyl diphosphate, for example, for the prenylation of lamins [26,29]. As FCS contains a certain amount of cholesterol/lipoproteins itself, this might influence the endogenous cholesterol biosynthesis and, thus, diminish the pathophysiological characteristics of primary human dermal fibroblasts of PXE patients *in vitro*. We, therefore, applied lipoprotein-depleted FCS, which contains a reduced amount of free cholesterol/lipoproteins compared to conventional FCS. Regarding control fibroblasts cultivated in 10% LPDS, we found no significant changes in gene expression for *LMNA*, *lamin C*, *progerin* or for *FNTB* and *ZMPSTE24* compared to control fibroblasts cultivated in 10% FCS. Neither did we see any obvious changes in the nuclei shape or protein expression and distribution of lamins between the different media for NHDF. Although Kuzaj *et al.* [21] showed that the 3hydroxy-3-methyl-glutaryl-coenzyme A reductase activity in NHDF cultivated in 10% LPDS is significantly elevated compared to the control fibroblasts cultivated in 10% FCS, this has obviously no influence on either the gene or protein expression of A-type lamins or the gene expression of LMNA-processing enzymes. By contrast, PXE fibroblasts cultivated under lipoprotein-depleted conditions showed a significant reduction of the gene expression of *LMNA* and *lamin C* compared to PXE fibroblasts cultivated in 10% FCS and control fibroblasts cultivated in 10% LPDS. A study of Miglionico *et al.* [30] also showed a reduction in the *LMNA/lamin C* gene expression in *ABCC6* knockdown HepG2 cells. However, they observed this downregulation in medium with 10% FCS. We only see this reduction under lipoprotein-depleted conditions, therefore, this strengthens the assumption that the exogenous cholesterol might diminish the pathophysiological characteristics of primary human dermal fibroblasts of PXE patients *in vitro*. However, *ZMPSTE24* gene expression and the immunofluorescence of LMNA/lamin C showed no significant changes for PXE fibroblasts at all, thus, it could be suggested that the documented induction of 3hydroxy-3-methyl-glutaryl-coenzyme A reductase activity and *farnesyl diphosphate synthase* gene expression in PXE fibroblasts compared to controls when cultivated under lipoprotein depleted conditions [21] only have a limited impact on A-type lamin protein expression and processing. It was also shown that the gene expression of *PCYOX* is significantly decreased in PXE fibroblasts compared to NHDF in lipoprotein-depleted medium [21]. As *PCYOX* is responsible for the degradation of prenylated proteins, its downregulation could be the result of a decrease of gene expression of prenylated proteins, as seen here for *LMNA* and *lamin C* gene expression, or the reduced mRNA expression of prenylated proteins, such as *LMNA* and *lamin C*, could be a direct result of the decreased *PCYOX* gene expression to avoid the accumulation of A-type lamins and, thus, ensure nuclear integrity. The overall downregulation of the *A-type lamin* gene expression could also be a reason for the decreased *progerin* and *FNTB* mRNA expression in PXE fibroblasts cultivated in 10% LPDS compared to those cultivated in 10% FCS.

In addition to the increased gene expression of *progerin*, it is known that HGPS fibroblasts show the alteration of other nuclear structures, such as the formation of nucleoli, important subcompartments of the nucleus. The HGPS fibroblasts show an enlarged nucleolar size, which is supposed to be an indicator of increased ribosome biogenesis and protein synthesis. Thus, several studies claimed nucleolar size itself as a hallmark of aging and premature aging processes [16,17]. We did not find any significant changes in the *NCL* gene or NCL protein expression between PXE fibroblasts and NHDF when cultivated in 10% FCS or 10% LPDS. Neither did we see any grave alteration of nucleolar size. These facts might indicate that aberrations of nucleolar organization probably play no or, at least, a secondary role in PXE pathogenesis.

It is also known that HGPS fibroblasts have significant shorter telomeres compared to the appropriate controls [18]. We, therefore, examined the telomere attrition by determining the relative telomere length of PXE fibroblasts compared to NHDF. Surprisingly, telomeres of PXE fibroblasts were significant longer than those of control fibroblasts when cultivated in 10% FCS. It has been shown previously that the telomere dysfunction in the case of HGPS is triggered by progerin [31]. Against the background that we have not seen a major increase in *progerin* expression for PXE fibroblasts, it seems to be reasonable that we also have not seen an accelerated telomere shortening in PXE fibroblasts comparable to those seen for HGPS fibroblasts. However, the fact that we observed longer telomeres in PXE fibroblasts compared to NHDF when cultivated in 10% FCS indicates that the kind of senescence which exist in PXE fibroblasts is not triggered by telomere length but is probably due to other factors. One possible stress factor could be a metabolic shift due to the induction of cholesterol biosynthesis mentioned above. This possibility is strengthened by the fact that we observed significantly shorter telomeres for PXE fibroblasts cultivated in 10% LPDS than those cultivated in 10% FCS. Thus, it could be the case that the PXE phenotype becomes more apparent when the cholesterol supply is limited to the endogenous synthesis. The lack of exogenous cholesterol might also have beneficial effects on PXE fibroblasts as it probably reduces the potential cholesterol excess and, thus, prevents a growth arrest, at least to a certain degree.

This is the first study evaluating relevant mechanisms known to be involved in HGPS pathogenesis in primary human dermal fibroblasts of PXE patients. However, in con-

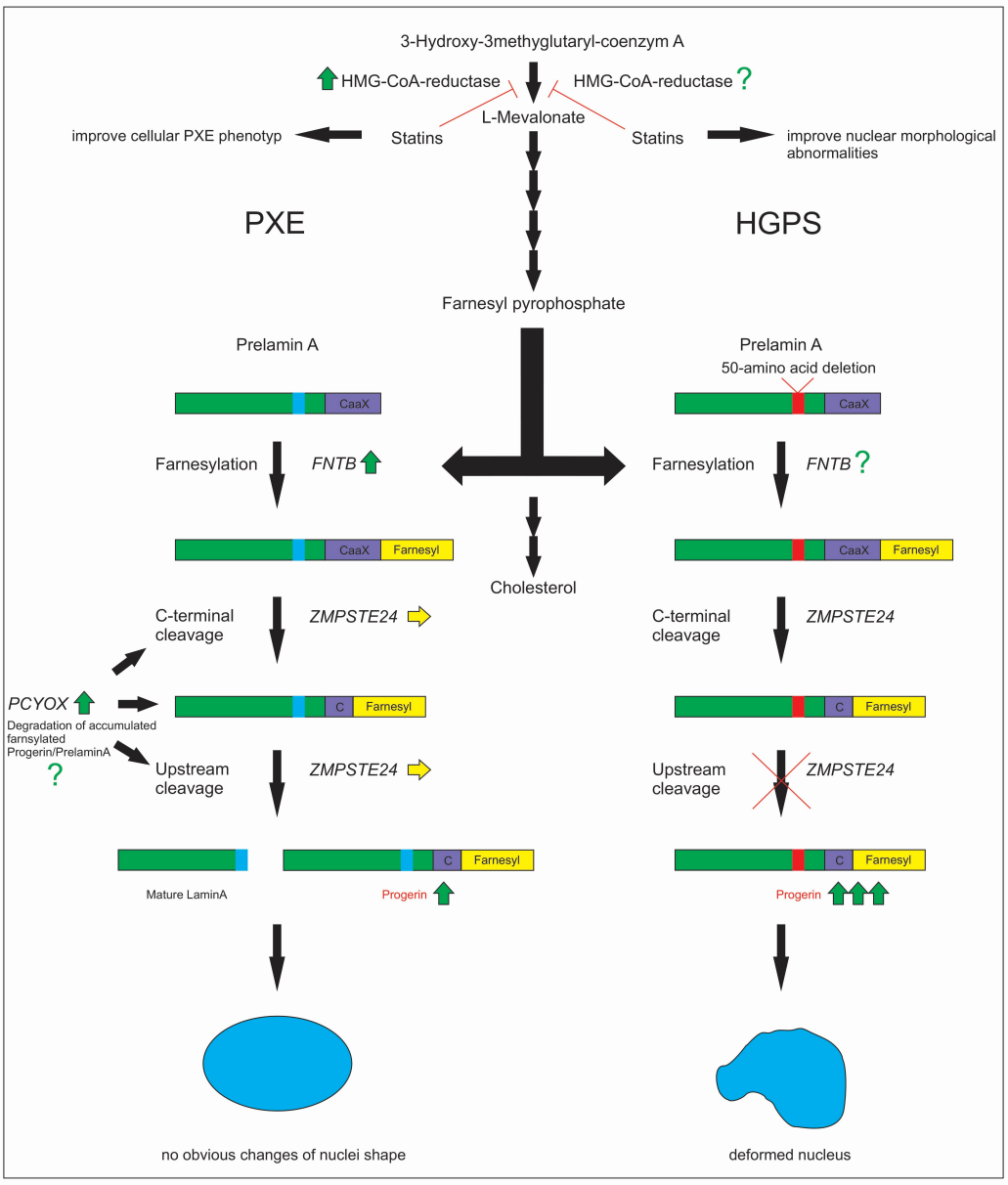

Fig. 5. Hypothetical scheme of farnesylation and processing of LMNA in PXE and HGPS. This scheme shows the cholesterol biosynthesis and downstream processing of LMNA in dermal PXE and HGPS. A key enzyme of cholesterol biosynthesis, HMG-CoA-reductase activity is increased in PXE fibroblasts [21] but unknown in HGPS, but therapy with statins seems to slow down progression in HGPS and in PXE [5,24]. Gene expression of *farnesyltransferase (FNTB), prenylcysteine oxidase 1* (*PCYOX*) and *progerin* is also increased (green arrow) in PXE fibroblasts, while *zinc metallopeptidase STE24* (*ZMPSTE24*) expression remains unchanged (yellow arrow). This indicates a persistent farnesylation of progerin, probably resulting in cellular senescence. However, changes of the nuclei shape were not observed in PXE fibroblasts. To the best of our knowledge, targets of the cholesterol synthesis pathway have not yet been investigated in HGPS. Due to mutations in the *LMNA* gene, farnesylated pre-LMNA cannot be cleaved by ZMPSTE24, resulting in high levels of progerin. The accumulation of progerin leads to deformed nuclei, which is the main reason for the pathogenesis of HGPS. The hypothetical scheme was modified according to Coutinho *et al.* [25].

trast to HGPS, the senescence in PXE fibroblasts observed was shown to be mostly independent of nuclear envelope defects or rearrangements of nucleoli.

5. Conclusions

In conclusion, our results indicate that neither changes in genomic integrity or telomer length, but rather metabolic aberrations seem to be the origin of senescent phenotype in PXE fibroblasts. Changes in A- and B-type lamins there-

for also appear to be complementary phenomena of these metabolic shifts, in particular by the induction of cholesterol biosynthesis.

Availability of Data and Materials

All data generated or analyzed during this study are available from the corresponding author on request.

Author Contributions

JT performed the experiments, data analysis, interpretation and manuscript writing. AB, CL, RP and TW helped with the experimental work. CK, DH and IFH contributed to the design of the study, data interpretation and manuscript preparation. All authors read and approved the final manuscript.

Ethics Approval and Consent to Participate

All patients and controls gave their informed consent for participation in the study. The study was conducted in accordance with the Declaration of Helsinki and approved by the Ethics Committee of the HDZ NRW, Department of Medicine, Ruhr University of Bochum (registry no. 32/2008).

Acknowledgment

We thank Christoph Lichtenberg for his excellent technical assistance. We are grateful to all the PXE patients and their relatives and the Selbsthilfegruppe für PXE Erkrankte Deutschlands e. V.

Funding

This work was supported by a FORUM research grant (grant number: K107-16) of the Ruhr-University Bochum.

Conflict of Interest

The authors declare no conflict of interest.

Supplementary Material

Supplementary material associated with this article can be found, in the online version, at https://doi.org/10.31083/j.fbl2803055.

References

[1] Germain DP. Pseudoxanthoma elasticum. Orphanet Journal of Rare Diseases. 2017; 12: 85.

[2] Legrand A, Cornez L, Samkari W, Mazzella JM, Venisse A, Boccio V, *et al*. Mutation spectrum in the ABCC6 gene and genotype-phenotype correlations in a French cohort with pseudoxanthoma elasticum. Genetics in Medicine. 2017; 19: 909–917.

[3] Ronchetti I, Boraldi F, Annovi G, Cianciulli P, Quaglino D. Fibroblast involvement in soft connective tissue calcification. Frontiers in Genetics. 2013; 4: 22.

[4] Gliem M, Zaeytijd JD, Finger RP, Holz FG, Leroy BP, Issa PC. An update on the ocular phenotype in patients with pseudoxanthoma elasticum. Frontiers in Genetics. 2013; 4: 14.

[5] Villa-Bellosta R, Rivera-Torres J, Osorio FG, Acín-Pérez R, Enriquez JA, López-Otín C, *et al*. Defective extracellular pyrophosphate metabolism promotes vascular calcification in a mouse model of Hutchinson-Gilford progeria syndrome that is ameliorated on pyrophosphate treatment. Circulation. 2013; 127: 2442–2451.

[6] Boraldi F, Annovi G, Vermeer C, Schurgers LJ, Trenti T, Tiozzo R, *et al*. Matrix Gla Protein and Alkaline Phosphatase are Differently Modulated in Human Dermal Fibroblasts from PXE Patients and Controls. Journal of Investigative Dermatology. 2013; 133: 946–954.

[7] Boraldi F, Annovi G, Bartolomeo A, Quaglino D. Fibroblasts from patients affected by Pseudoxanthoma elasticum exhibit an altered PPi metabolism and are more responsive to procalcifying stimuli. Journal of Dermatological Science. 2014; 74: 72–80.

[8] Liu C, Arnold R, Henriques G, Djabali K. Inhibition of JAK-STAT Signaling with bariticinib reduces inflammation and improves cellular homeostasis in progeria cells. Cells. 2019; 8: 1276.

[9] Tiemann J, Wagner T, Lindenkamp C, Plümers R, Faust I, Knabbe C, *et al*. Linking ABCC6 deficiency in primary human dermal fibroblasts of PXE patients to p21-mediated premature cellular senescence and the development of a proinflammatory secretory phenotype. International Journal of Molecular Sciences. 2020; 21: 9665.

[10] Varela I, Pereira S, Ugalde AP, Navarro CL, Suárez MF, Cau P, *et al*. Combined treatment with statins and aminobisphosphonates extends longevity in a mouse model of human premature aging. Nature Medicine. 2008; 14: 767–772.

[11] Guo H, Li Q, Chou DW, Uitto J. Atorvastatin counteracts aberrant soft tissue mineralization in a mouse model of pseudoxanthoma elasticum (Abcc6 −/−). Journal of Molecular Medicine. 2013; 91: 1177–1184.

[12] Luft FC. Pseudoxanthoma elasticum and statin prophylaxis. Journal of Molecular Medicine. 2013; 91: 1129–1130.

[13] Li Q, Sundberg JP, Levine MA, Terry SF, Uitto J. The effects of bisphosphonates on ectopic soft tissue mineralization caused by mutations in the ABCC6 gene. Cell Cycle. 2015; 14: 1082–1089.

[14] McClintock D, Ratner D, Lokuge M, Owens DM, Gordon LB, Collins FS, *et al*. The mutant form of lamin A that causes Hutchinson-Gilford progeria is a biomarker of cellular aging in human skin. PLoS ONE. 2007; 2: e1269.

[15] Cao K, Blair CD, Faddah DA, Kieckhaefer JE, Olive M, Erdos MR, *et al*. Progerin and telomere dysfunction collaborate to trigger cellular senescence in normal human fibroblasts. Journal of Clinical Investigation. 2011; 121: 2833–2844.

[16] Buchwalter A, Hetzer MW. Nucleolar expansion and elevated protein translation in premature aging. Nature Communications. 2017; 8: 328.

[17] Tiku V, Jain C, Raz Y, Nakamura S, Heestand B, Liu W, *et al*. Small nucleoli are a cellular hallmark of longevity. Nature Communications. 2017; 8: 16083.

[18] Allsopp RC, Vaziri H, Patterson C, Goldstein S, Younglai EV, Futcher AB, *et al*. Telomere length predicts replicative capacity of human fibroblasts. Proceedings of the National Academy of Sciences of the United States of America. 1992; 89: 10114–10118.

[19] Decker ML, Chavez E, Vulto I, Lansdorp PM. Telomere length in Hutchinson-Gilford Progeria Syndrome. Mechanisms of Ageing and Development. 2009; 130: 377–383.

[20] Aubert G, Lansdorp PM. Telomeres and Aging. Physiological Reviews. 2008; 88: 557–579.

[21] Kuzaj P, Kuhn J, Dabisch-Ruthe M, Faust I, Götting C, Knabbe C, *et al*. ABCC6- a new player in cellular cholesterol and

lipoprotein metabolism? Lipids in Health and Disease. 2014; 13: 118.

[22] Gibson K, Hoffmann G, Schwall A, Broock R, Aramaki S, Sweetman L, *et al*. 3-Hydroxy-3-methylglutaryl coenzyme a reductase activity in cultured fibroblasts from patients with mevalonate kinase deficiency: differential response to lipid supplied by fetal bovine serum in tissue culture medium. Journal of Lipid Research. 1990; 31: 515–521.

[23] Rodriguez S, Coppedè F, Sagelius H, Eriksson M. Increased expression of the Hutchinson–Gilford progeria syndrome truncated lamin a transcript during cell aging. European Journal of Human Genetics. 2009; 17: 928–937.

[24] Tiemann J, Lindenkamp C, Plümers R, Faust I, Knabbe C, Hendig D. Statins as a therapeutic approach for treatment of Pseudoixanthoma elasticum patients: evaluation of the spectrum efficacy of atorvastatin *in vitro*. Cells. 2021; 10: 442.

[25] Coutinho HDM, Falcão-Silva VS, Gonçalves GF, da Nóbrega RB. Molecular ageing in progeroid syndromes: Hutchinson-Gilford progeria syndrome as a model. Immunity & Ageing. 2009; 6: 4.

[26] Scott Reid T, Terry KL, Casey PJ, Beese LS. Crystallographic Analysis of CaaX Prenyltransferases Complexed with Substrates Defines Rules of Protein Substrate Selectivity. Journal of Molecular Biology. 2004; 343: 417–433.

[27] Hunag J, Ralph D, Boraldi F, Quaglino D, Uitto J, Li Q. Inhibition of DNA damage response attenuates ectopic calcification in Pseudoxanthoma elasticum. Journal of Investigative Dermatology. 2022; 142: 2140–2148.e1.

[28] Ibold B, Faust I, Tiemann J, Gorgels TGMF, Bergen AAB, Knabbe C, *et al*. Abcc6 deficiency in mice leads to altered ABC transporter gene expression in metabolic active tissues. Lipids in Health and Disease. 2019; 18: 2.

[29] Schreiber K, Kennedy B. When Lamins Go Bad: Nuclear Structure and Disease. Cell. 2013; 152: 1365–1375.

[30] Miglionico R, Ostuni A, Armentano MF, Milella L, Crescenzi E, Carmosino M, *et al*. ABCC6 knockdown in HepG2 cells induces a senescent-like cell phenotype. Cellular & Molecular Biology Letters. 2017; 22: 7.

[31] Benson EK, Lee SW, Aaronson SA. Role of progerin-induced telomere dysfunction in HGPS premature cellular senescence. Journal of Cell Science. 2010; 123: 2605–2612.